JOURNAL OF PROPULSION AND POWER
Vol. 25, No. 2, March–April 2009

Production, Characterization, and Combustion of Nanoaluminum in Composite Solid Propellants

K. Jayaraman,* K. V. Anand,† D. S. Bhatt,* S. R. Chakravarthy,‡ and R. Sarathi§
Indian Institute of Technology—Madras, Chennai 600 036, India

DOI: 10.2514/1.36490

This paper reports the production of nanoaluminum particles using the wire explosion process at our laboratory. Electrical energy is applied to the aluminum wire in an argon atmosphere to yield spherical particles around 50 nm in size. The material is also characterized by a number of methods. The nano-Al is included in bimodal ammonium perchlorate composite solid propellants, and their burning rates are compared with those containing normal micron-sized aluminum and nonaluminized propellants in a total of 21 formulations in the 1–12 MPa pressure range. Nanoaluminized propellants show ∼100% increase in burning rate relative to nonaluminized or microaluminized ones, but only when large-sized coarse ammonium perchlorate particles are used. Burning-rate plateaus observed in non- and microaluminized propellants are washed out with the addition of nano-Al, but the burning rates of nanoaluminized propellants register low pressure exponents in the elevated pressure range. The results suggest that the heat feedback from the diffusion-limited combustion of nano-Al particles near the propellant burning surface controls the propellant burning rate when sufficiently large parts of the burning surface are made up of the nanoaluminized fine ammonium-perchlorate/binder matrix.

I. Introduction

ALUMINUM powder of nanometric particle size has been gaining attention in recent times as a potential ingredient in solid propellant rockets, guns, explosives, thermites, etc. In the context of rocket propulsion, the use of nanoaluminum (nAl) offers the possibility of an increased specific impulse because of reduced two-phase losses to thrust, despite the increased content of aluminum oxide in the powder. In judicious combination with micron-sized aluminum of appropriate size, it could enable finer control of particulate damping of combustion instability in solid rockets by reducing the agglomeration of the latter to a significant extent.

The use of "ultrafine" aluminum of particle size ∼100 nm or above in the combustion of solid propellants was reported relatively early in the literature [1]. In recent times, a plethora of papers are appearing on this subject. Ivanov et al. [2] reported the production of ultrafine powders of different metals including aluminum by the electrical wire explosion process. They reported the generation of aluminum particles of mean sizes in the 30–50 nm range. Lee et al. [3] reported the production of nAl powder by a similar technique in the size range of 80–120 nm.

Many researchers reported working with nAl samples obtained from different commercially available sources and some Russian universities. These sources adopt different methods for the production of nAl, such as the pulsed plasma technique, vapor condensation, etc., besides the electroexplosion technique. The particles from these different sources are over a relatively wide range of mean sizes, 24–500 nm, mostly in relation to the method of production. Particles produced by the electrical wire explosion method, popularly termed "Alex" and widely studied/reported on, are typically ∼100–200 nm in size, except for what has been reported by Ivanov et al. [2] so far.

Thermal analyses such as thermogravimetric analysis (TGA), differential thermal analysis (DTA), and differential scanning calorimetry of nAl samples were performed and contrasted with the characteristics of micron-sized aluminum samples by several investigators [4–8]. Some other investigators examined the role of nAl in the thermal decomposition of other propellant/explosive ingredients, such as ammonium perchlorate (AP) [9] and cyclotrimethylenetrinitramine (RDX) [5,10]. The important pertinent results of these investigations are as follows: 1) nAl melts at a lower temperature than the melting point of bulk aluminum, 2) the oxidation of nAl commences at quite low temperatures, and 3) the low-temperature decomposition of AP is accelerated in the presence of nAl. The last result supports the observation of extraordinarily high burning rates of pressed pellets of dry mixtures of AP and ultrafine aluminum (UFAl) reported earlier in [1]. DeSena and Kuo [11] examined the possibility of stored energy due to rapid solidification in the formation of ultrafine exploded aluminum particles and found it to be negligible. Trunov et al. [8] explained the mechanism of oxidation of nAl in the framework of the staged oxidation and ignition of micron-sized aluminum particles and associated crystalline phase changes of the formed oxide, as in earlier works [12,13]. Rai et al. [14] examined the oxidation of nAl particles with mass spectrometry, transmission electron microscopy, and density measurements. They highlight the role of the diffusion of oxygen across the oxide skin in nAl particles, which is slow before the melting of the aluminum but rapid thereafter. Kwon et al. [15] combusted dusts of UFAl in air to find a prominent role for the formation of aluminum nitride from the nitrogen in the air along with aluminum oxide formation. Huang et al. [16] combusted particle clouds of bimodal blends of nano- and micron-sized aluminum particles in air and reported higher flame speeds of the nano-Al/air flame when compared with the micron-sized Al/air flame. For smaller quantities of nAl in the blend of both sizes, two distinct flame zones exist, but for larger quantities of it, a merger of the two flame zones is evident.

Some investigators devoted attention to the aspect of effecting surface coatings on nAl particles for passivation and have characterized such coated particles. Jones et al. [17] and Kwok et al. [18] reported the characterization of nAl particles of different sizes coated with a thicker oxide layer, a fluoropolymer, etc. They also investigated the thermal behavior of such particles in combination with other energetic materials, such as RDX, trinitrotoluene, AP, etc.

Received 6 January 2008; revision received 21 September 2008; accepted for publication 21 September 2008.

*Ph.D. Scholar, Department of Aerospace Engineering.
†M.S. Scholar, Department of Aerospace Engineering; currently at Tata Consultancy Services, Chennai, India.
‡Associate Professor, Department of Aerospace Engineering; src@ae.iitm.ac.in.
§Associate Professor, Department of Electrical Engineering.

Bocanegra et al. [19] compared the burning times of micron-sized Al, uncoated and coated with nickel, with those of UFAl powders obtained from several Russian sources. They found that both the Ni-coated micron-sized aluminum and UFAl have decreased burn times, but the latter burn still faster. Dubois et al. [20] reported the coating of nAl and boron particles by grafting polyethylene-type polymers and polyurethane onto the metal powders and characterized the resulting materials.

Many studies investigated the effect of UFAl on the burning rates of composite solid propellants, particularly those based on AP. As mentioned earlier, Romonadova and Pokhil [1] reported burning rates of dry-pressed mixtures of AP and UFAl. Pai Verneker et al. [21] sought to explain the results based on the variation of the heat of combustion of the AP–Al reaction with a composition of such mixtures. Dokhan et al. [22] examined the burning rates of propellant compositions up to 6.9 MPa, with unimodal ultrafine or micron-sized aluminum particles as well as bimodal combinations of the particles of both sizes. They reported that the addition of UFAl increases the burning rate of the propellant through ignition of the aluminum particles by the leading-edge flames (LEFs) over the coarse AP/binder interfaces and/or the flames of the fine AP/binder matrix. Ivanov et al. [2] also reported increases in burning rates with nAl by about 1.6–2 times relative to nonaluminized propellant compositions at different pressures and levels of aluminum addition. De Luca et al. [23] and Galfetti et al. [24,25], among other tests, reported most importantly on the burning rates of propellants containing UFAl in comparison with those without it over a pressure range of up to 7 MPa. They found that the burning rates nearly double with the addition of UFAl uniformly across the test range of pressures, that is, without any change in the pressure exponent of that burning rate averaged over the entire test pressure range. These studies also tested bimodal blends of aluminum in some propellant formulations, with results that are similar to that of Dokhan et al. [22]. Pivkina et al. [26] reported the production of nanosized AP as well as nanosized aluminum containing 10% graphite by the method of mechanical activation in the size ranges of 35–100 nm for the former and 20–50 nm for the latter. They combusted AP–Al mixtures approximately in the ratio of 76:24 over the 1–6 MPa pressure range, and found that the replacement of micron-sized (10 μm) AP by nanosized AP alone did not significantly alter the burning rate or its pressure exponent. Replacement of micron-sized (97 μm) Al by nAl alone increased the burning rate by >5 times, but without altering the pressure exponent. The simultaneous replacement of both micron-sized AP and Al by nanosized AP and AL caused an over tenfold increase in the burning rate relative to their micron-sized counterpart mixtures and also nearly halved the pressure exponent averaged across the entire test pressure range. Popenko et al. [27] reported an increase in burning rates and a decrease in pressure exponents of condensed systems of high-molecular-weight RDX with small quantities (1.25–5%) of UFAl powders. They noted that no adverse effect was observed on the rheological properties of the model propellants because of such an addition. Dokhan [28] and Galfetti et al. [24,25] reported studying the agglomeration of UFAl during the combustion of a propellant containing such particles. Karasev et al. [29] further studied the structure of aggregates of aluminum oxide formed in the combustion of UFAl in air. These studies affirmed that agglomerates of UFAl or their combustion products do not exceed a few micrometers in size, an aspect of practical interest in solid rocket propulsion.

Among the many methods of producing nanoparticle-sized metal powders, the electrical wire explosion technique consumes relatively low levels of energy. It is estimated at ~4 kWh/kg, although lower estimates at around half this value were also reported earlier [30]. Our laboratory has been involved in the development of procedures for generating nanometal powders by the electrical wire explosion technique in recent years. Sabari Giri et al. [31] reported the generation of nano-Al_2O_3 by the explosion of an aluminum wire in air ambience. Sarathi et al. [32] reported the material characterization of nano-Al_2O_3 and high-speed imaging of the explosion event to understand the mechanism of nanoparticle formation by the wire explosion technique. Sindhu et al. [33] reported the production of nano-AlN by explosion of aluminum wire in a nitrogen ambience. Sarathi et al. [34] reported the generation and characterization of nAl metal particles by the explosion of wires of that material in different inert ambiences, such as nitrogen, argon, and helium. Sindhu et al. [35] reported the effect of pressure of the ambient medium on the size distribution and other material characterization features of nAl particles obtained in different ambiences. In a novel approach, Sarathi et al. [36] explored the use of binary mixtures of inert gases for the ambience in influencing the particle size and other characteristics of nAl powders. All these works have enabled the control of the peak in the size distribution of the produced nanoparticles within the 20–50 nm range over a spread of 0–100 nm. The total cost of production of nAl at this laboratory, including the cost of aluminum wire and power consumption, is estimated to be ~US6.3/kg. Sindhu et al. [37] modeled the process of nucleation and coagulation of vaporized aluminum following the wire explosion and simulated the population dynamics of particles to obtain the late time size distribution in different ambiences. The model predictions agree well with the experimental results in terms of the size distributions and also support the partial formation of irregular-shaped particles in a nitrogen ambience due to nitration of the surface of the particles. A similar modeling effort including a Monte Carlo simulation accounting for the exothermic nature of particle coalescence was also reported by Mukherjee et al. [38].

The aforementioned work was performed in this laboratory only on a single-wire/single-shot mode at the level of producing a few tens of milligrams of nanoparticles. Therefore, a new setup has also been developed to sequentially explode multiple wires per batch, so that the yield is improved to the gram level for application in solid propellants. The present paper reports the production and characterization of nAl in the new setup and the use of this material in propellant compositions. Comparisons of burning rates of nanoaluminized propellant formulations are made with those of nonaluminized formulations and those containing micron-sized aluminum particles, referred to here as microaluminized formulations, altogether totaling 24 propellant formulations in the pressure range of 1–12 MPa. All the formulations contain a bimodal size distribution of AP particles. These formulations are based on propellants with bimodal AP size distribution exhibiting plateau-burning-rate trends in the intermediate pressure range of ~4–6 MPa [39] and in the elevated pressure range of ~10–14 MPa [40]. The intermediate-pressure plateau was shown to be related to the midpressure self-extinction of the fine AP/binder matrix because of binder-melt flow effects [39]. The elevated pressure plateau is due to the diminishing lateral extent of the LEFs over the coarse AP particles and the contribution from the outer diffusion flame at elevated pressures [40]. Recently, Banerjee and Chakravarthy [41] reported the testing of 10 such propellant formulations, some of which exhibit multiple plateau/mesa trends in the 1–12 MPa pressure range. These propellants typically use fine and coarse AP particles, whose sizes are widely separated, with the fine AP particles specifically in the 5–20 μm size range. These propellants also use isophorone di-isocyanate as the curing agent for the hydroxyl-terminated poly-butadiene (HTPB) binder, which is shown to involve melt flow effects [38]. The binder-melt flow leads to midpressure extinction of the fine AP/binder matrices [39,41] for the fine AP size range already noted, depending upon the fine AP content in the matrix [41]. Because the focus of the present work is on the effect of the addition of nAl on propellant burning rates, an attempt is made to move away from the regime of plateau burning by 1) switching to toluene di-isocyanate (TDI) for the curing agent, which is noted to produce less binder-melt flow effects; 2) using larger-sized fine AP particles than in the aforementioned works; and 3) reducing the size of the coarse AP as well. All the formulations reported in the present work are with the TDI curative, and the separation between the sizes of the fine and coarse AP particles is varied. Therefore, on the whole, propellant formulations with a wide range of pressure exponents in different pressure ranges are nanoaluminized in the present study. A comparison of the burning rates of the nano- and microaluminized fine AP/binder matrices is also made, in this context. This approach lends itself to examining the burning-rate controlling mechanism in nanoaluminized propellants

in terms of how the pressure exponent of the burning rate changes with the inclusion of nAl. Data have been obtained in close intervals of pressure so as to track changes in the pressure exponent in different pressure ranges, unlike in the previous literature [23–25]. Other works on propellant combustion with nano- or UFAl particles [2,22] do not concern themselves with the variation of the pressure exponent in different pressure ranges and its implication on the physical mechanism that controls the burning rate.

II. Experimental Details

A. Generation of Nanoaluminum (ALEX) Particles

The experimental setup consists of an electrical circuit, wire explosion chamber, and particle collection chamber. The electrical section consists of diodes, capacitors (3 μF), a switch, and the controlling device. The wire explosion chamber (Fig. 1) consists of provisions for fixing the wire, the inlet and exit of the vacuum and required gas medium, pressure gauges, pressure valves, and the main chamber. The collection chamber consists of the prefilter, main filter, and postfilter. The filters are mounted at the bottom of the exploding chamber, primarily to collect the nAl particles. Initially, multiple aluminum wires of 0.42 mm in diameter and 140 mm in length each are connected between the electrical contacts, and the chamber is evacuated in the range of 700 mm of Hg. Then, the chamber is purged and filled with argon gas (>99% purity) at 1 bar gauge pressure to prevent oxidation of the powder. The capacitor is charged to 24 kV, the switch is closed, and the capacitor is discharged. After explosion of all the wires is completed, the inert gas is sent out through the top of the chamber and the nAl powder is collected at the filter. Superheating of the evaporated material determines the particle size in the wire explosion process. The particle size produced by the wire explosion process reduces substantially with increasing superheating of the metal. The extent of superheating is determined by the factor $k = W/W_s$, where W is the energy injected into the evaporating wire and W_s is the sublimation energy for the wire. The sublimation energy diminishes with the reduction in diameter of the wire [34]; for aluminum, it is 33 J/mm^3. For the present experimental conditions, the value k is maintained at 1.14.

B. Methods of Nanoaluminum Characterization

The particle size measurement is carried out by the transmission electron microscopic (TEM) analysis of the bright field images. The size of a particle is determined from the area of the particle in the image. The atomic composition is obtained from energy dispersive x-ray (EDAX) analysis. Wide-angle x-ray diffraction (WAXD) measurements are performed using a Phillips x-ray diffractometer. A scan rate of 2 deg / min at 2000 cycles using Cu Kα radiation of wavelength 1.5426 Å applied. A radial scan of diffraction angle (2θ) vs intensity is obtained with an accuracy of ± 0.25 deg at the location of the peak. The TGA–DTA studies are done with Netzch STA 409C equipment. These experiments are performed in a nitrogen atmosphere in the range of 25–750°C at a heating rate of 10°C/ min.

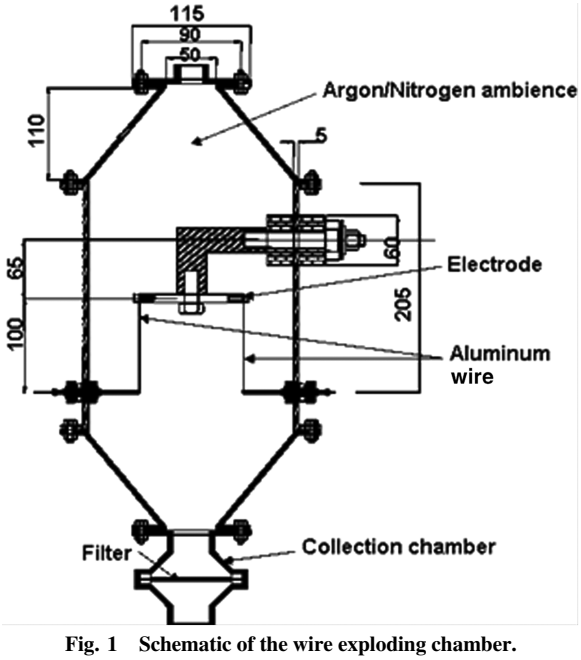

Fig. 1 Schematic of the wire exploding chamber.

C. Propellant Ingredients and Samples

The AP used in the present work is obtained from Tamilnadu Chlorates, Madurai, India. The purity of the AP is >99%, and it does not contain any anticaking agents. The oxidizer particles are subjected to grinding in a vibratory rod mill to reduce the size. The ground particles are size segregated using a standard set of sieves down to 37 μm. For further size reduction, a tabletop fluid energy mill is used with its settings calibrated to obtain the desired size range of the particles. Four size ranges of fine AP are used in the propellant formulations, designated as 5, 20, 53, and 75 μm. The coarse AP particles used in the propellant formulations are median sized at 450, 350, and 250 μm. The micro-Al (μAl) used in comparison studies is obtained from the Metal Powder Company, Madurai, India. It is nominally 15 μm in size, mostly nonspherical in shape but not in the form of flakes. Particle size distributions are obtained with the help of an optical microscope and the digital image processing of nearly 1000 particles of a powder sample. The size distributions of all micron-sized powders used in the present work are shown in Fig. 2. The binder is made of HTPB cured by TDI, with the addition of dioctyl adipate (DOA) as a plasticizer during mixing. The proportions are 80% HTPB, 15% DOA, and 5% TDI. All the propellants contain 87.5% total solids and 12.5% binder. In the case of aluminized propellants, 15% aluminum is used in place of coarse AP particles, so that the fine AP/binder ratio as well as the total solids is maintained for comparison. Three families of formulations are considered with a fixed fine AP/binder ratio (60/40) for each case, that is, non-aluminized, nanoaluminized, and micro-aluminized: 1) a coarse AP size of 450 μm and fine AP sizes of 5, 20, 53, and 75 μm; 2) a coarse AP size of 350 μm and fine AP sizes of 5 and 75 μm; and 3) a coarse AP size of 250 μm and fine AP sizes of 5 and 75 μm. The propellant formulations tested in the present study are listed in Table 1. Propellants are prepared first by weighing the ingredients to within a 1% error and hand mixing them thoroughly for 30 min; the mixture is then transferred and mixed for 30 min in a micromixer developed in-house. The mixture is then vacuum cast into a container, in which a plunger is used to close blowholes during evacuation. The propellants are cured for 1 week at 50°C. Propellant samples are of the approximate dimensions of $5 \times 5 \times 12$ mm, which is appropriate following previous studies [42]. A thin layer of silicon grease is applied on the sides of the propellant sample, which prevents the sample from burning down the sides. Ignition is achieved by passing electric current through a Nichrome wire along the top surface of the sample. To achieve uniform flame spread during ignition, a thin layer of rubber solution is smeared over the Nichrome wire on the top surface, following previous studies [22].

D. Combustion Experiments

1. Measurement of Heat of Combustion

Heats of combustion at a constant volume of propellants with different compositions are measured in a standard bomb calorimeter. The apparatus consists of a stainless steel pressure vessel in which the sample is placed, pressurized by nitrogen to 0.5 MPa, and ignited. The pressure vessel is placed in a water bath that is constantly stirred, and its temperature is measured by a Beckman thermometer. Applying the principle of calorimetry, the heat released during the combustion of known quantity of the sample is determined from the temperature rise of the surrounding water, after adjusting for the thermal capacity of the apparatus.

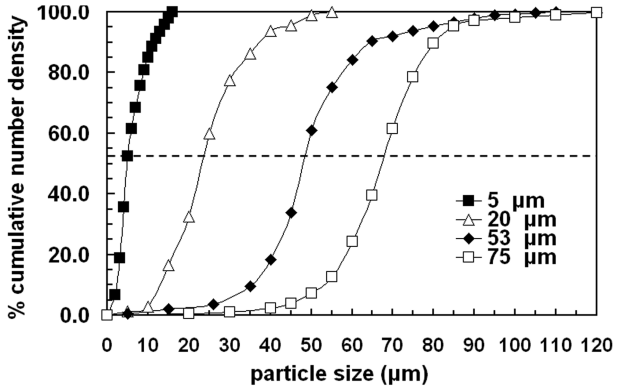

a) Fine AP

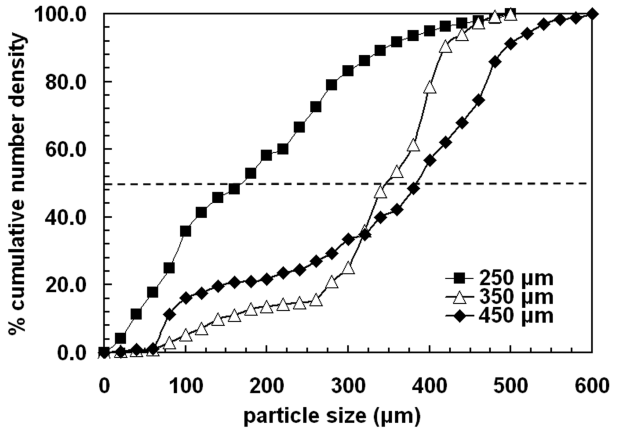

b) Coarse AP

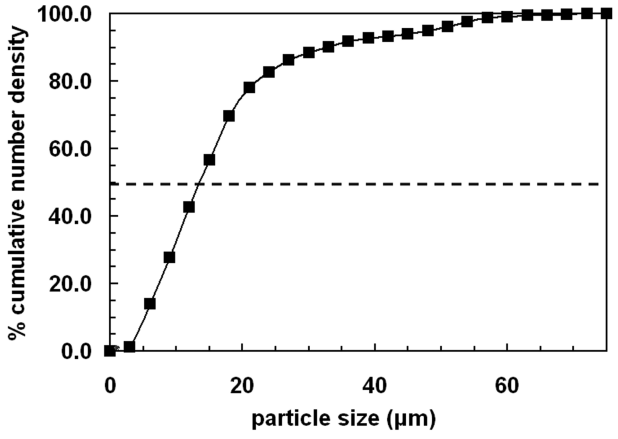

c) Aluminum

Fig. 2 Size distributions of micron-sized powders used in the present study.

2. Burning-Rate Measurement

Combustion photography is adopted for the burning-rate measurement. A window bomb is used for this purpose; it is a pressure vessel with two windows, one to illuminate the sample and another to view the combustion process with the help of a video camera. The video recording of the combustion event is played frame by frame, and the burning surface is marked in each frame along a line in the overall direction of the average surface regression. A straight line is fitted to the loci of the burning surface plotted against the framing time to a correlation of >99%; the slope of the straight line, adjusted for magnification of the video images, gives the burning rate. The uncertainty in measuring the burning rate with the window bomb is determined as ±3%. Nearly 70% of the tests are repeated at least once, and burning rates obtained within a repeatability of 5% are considered acceptable.

III. Results and Discussion

A. Characterization of Nano-Al

Figure 3 shows a TEM image of nAl powder produced in argon ambience. It can be seen that the shape of the particles is spherical. Images such as these are used to obtain the particle size distribution of the produced nanopowder, shown in Fig. 4. The peak size in the distributive distribution as well as the 50% size in the cumulative distribution seen in Fig. 4 is ∼52 nm. This is similar to that reported by Ivanov et al. [2] from the electroexplosion technique, but unlike the larger sizes (∼80–180 nm) of samples produced by this technique and supplied to most other investigators. The latter samples were, therefore, more appropriately termed as UFAl rather than nAl.

Figure 5 shows the x-ray diffraction pattern of nAl powder obtained in the present work. The first two dominant peaks correspond to the presence of aluminum in the sample; it can be observed that the purity of the sample is high. The results of the EDAX, shown in Fig. 6, indicate a 93.5 wt% of atomic aluminum and a 6.5 wt% of atomic oxygen of the nAl powder produced in argon ambience. This implies 86.2% of aluminum and 13.8% of Al_2O_3, assuming only those two compounds to be present in the samples. The relatively high content of aluminum oxide is obviously because of the high surface area of the nAl powder. The aluminum oxide layer thickness is estimated as 1.35 nm, assuming the spherical shape of particles and considering the equivalent masses of Al and Al_2O_3.

Figure 7 shows TG–DTA plots of nAl powder produced in argon ambience. These experiments, however, are performed in nitrogen ambience. The exotherms and mass gains observed in the TG–DTA results show the thermal runaway of nitration of nAl powders [18]. The peak in the DTA curve at ∼650°C shows that the melting point of nAl is slightly low when compared with that of bulk aluminum. The TGA shows 12% increase in mass, which represents high reactivity of nAl, as observed by previous researchers.

B. Heats of Combustion of Propellant Compositions

Considering the expectedly rather high level of oxide in the nAl powder produced, the corresponding loss in performance of the propellant formulations containing that ingredient is examined here. The theoretical specific impulse of a rocket motor using any of the three formulations (non-, micro-, and nanoaluminized) is estimated, taking into account that 13.8% of the nAl contains Al_2O_3. In contrast, the aluminum oxide present in the microaluminized propellant is neglected in the calculations in the present work, as is usually the practice. The theoretical calculations are performed with the CEA-400 code [43,44]. The calculations are made for a chamber pressure of 7 MPa with a nozzle area ratio of 8.5. The results of the theoretical performance calculations are shown in Table 2. It can be seen that the decrease in the specific impulse, because of including a relatively large amount of aluminum oxide as part of the nanoaluminized propellant as opposed to none for the microaluminized propellant, is ∼1.5%.

To verify if this theoretical result is reflected in practice, the heats of combustion of three propellants, non-, micro-, and nanoaluminized formulations, are measured using the bomb calorimeter. These propellants use 450 μm coarse AP and 20 μm fine AP. The results are presented in Table 3. It can be seen that both the aluminized formulations exhibit notably higher heats of combustion than the nonaluminized one, as expected. The heat of combustion of the nonaluminized sample, in particular, is of the same order as that reported by Kishore et al. [45]. Between the two aluminized samples, the heat of combustion of the nanoaluminized propellant is reduced from that of the microaluminized one by ∼1.7%, which is slightly greater than observed in the aforementioned theoretical calculations. Motor firing tests would involve substantial two-phase flow losses to thrust and specific impulse with microaluminized propellants than with the nanoaluminized ones. It could be expected that the decrease in the specific impulse with μAl is more than the slight decrease from of the larger amount of aluminum oxide in the nAl, as pointed out in the Introduction.

Table 1 Propellant formulations tested in the present study

S. no.	Al size, μm/nm	Al% in propellant	Coarse AP size, μm	Fine AP size, μm	Coarse AP% in propellant	Coarse/fine AP ratio
1	——	——	450	5	68.75	3.66
2	15 μm	15	450	5	53.75	2.86
3	50 nm	15	450	5	53.75	2.86
4	——	——	450	20	68.75	3.66
5	15 μm	15	450	20	53.75	2.86
6	50 nm	15	450	20	53.75	2.86
7	——	——	450	53	68.75	3.66
8	15 μm	15	450	53	53.75	2.86
9	50 nm	15	450	53	53.75	2.86
10	——	——	450	75	68.75	3.66
11	15 μm	15	450	75	53.75	2.86
12	50 nm	15	450	75	53.75	2.86
13	——	——	350	5	68.75	3.66
14	15 μm	15	350	5	53.75	2.86
15	50 nm	15	350	5	53.75	2.86
16	——	——	350	75	68.75	3.66
17	15 μm	15	350	75	53.75	2.86
18	50 nm	15	350	75	53.75	2.86
19	——	——	250	5	68.75	3.66
20	15 μm	15	250	5	53.75	2.86
21	50 nm	15	250	5	53.75	2.86
22	——	——	250	75	68.75	3.66
23	15 μm	15	250	75	53.75	2.86
24	50 nm	15	250	75	53.75	2.86

C. Burning Rates of Fine AP/Binder Matrices

The burning rates of fine AP/binder matrices alone, that is, without the coarse AP particles as would be in a propellant, are examined in Fig. 8 for the fine AP sizes of 5 and 20 μm. Nonaluminized matrices with fine AP particles of these two sizes, among those tested, show midpressure extinction or no burning at all within the test pressure range. The proportion of aluminum and the fine AP/binder mixture in the aluminized matrices is the same as in the propellants tested in the present study. As can be seen from Fig. 8, the nonaluminized 5 μm fine AP matrix does not burn in the entire test pressure range and the nonaluminized 20 μm fine AP matrix does not burn at low and intermediate pressures. But, the micro-aluminized and nanoaluminized matrices with fine AP particles of both size burn in the entire test pressure range. The LEFs anchored over the interfaces between the coarse AP particles and the fine AP/binder matrix in propellants (at full solids loading) are the principal sources of ignition of micron-sized aluminum particles and their accumulates [22,46–49]. The fine particles are too small and/or the pressure is sufficiently low for LEFs to be attached to them [50]. Here, the microaluminized matrix with 5 μm fine AP burns, albeit at relatively low burning rates, when its nonaluminized counterpart does not; similarly, the microaluminized 20 μm fine AP matrix burns at low pressures whereas its nonaluminized counterpart does not. This shows that the presence of the μAl causes the fine AP/binder matrix to burn. The matrix flame obviously acts as the source of ignition of the aluminum particles and their accumulates in the absence of the LEFs over matrix/coarse AP particle interfaces, as would be the case in propellants. The matrix

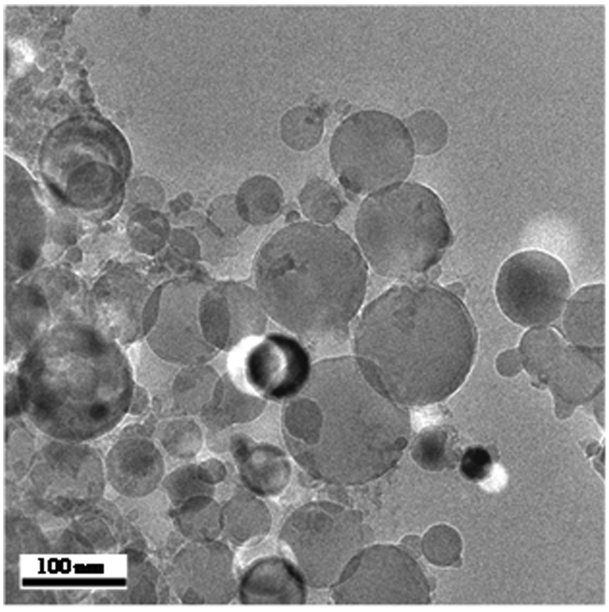

Fig. 3 TEM image of nAl.

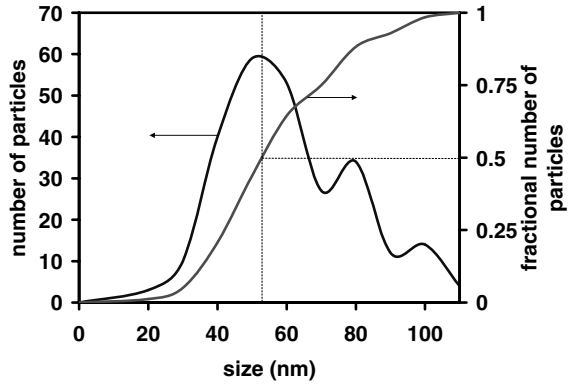

Fig. 4 Distributive (left ordinate) and cumulative (right ordinate) size distributions of nAl particles obtained in argon ambience.

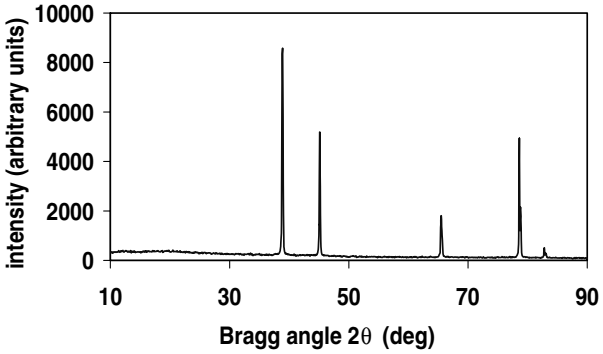

Fig. 5 X-ray diffraction pattern of nAl.

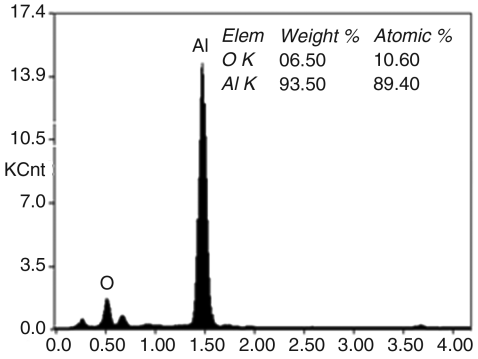

Fig. 6 EDAX results of nAl.

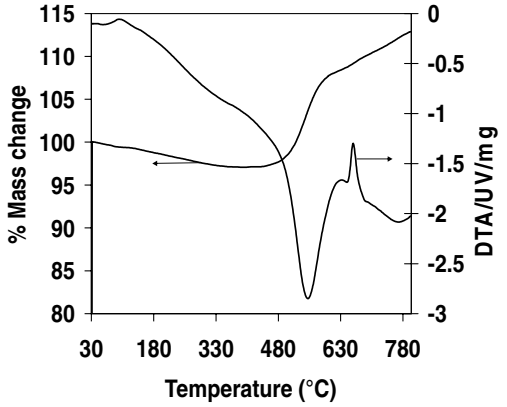

Fig. 7 TG–DTA of nAl.

flame is most probably premixed, particularly for the 5 μm fine AP particle size and pressure range under consideration. It is possible that aluminum particles get ignited from the flame of the ignition charge during the ignition of the matrix sample and that the aluminum flame aids in sustaining a fine AP/binder flame before leaving the vicinity of the surface. This is possible because the quantity of aluminum particles is relatively large in proportion to the rest of the matrix, as their proportions are retained the same as in the propellants. The matrix flame, thus assisted, in turn, ignites other aluminum particles accumulating on the burning surface subsequently, and the interaction continues. In fact, the synergistic combustion between the aluminum and the fine AP/binder matrix leads to increased burning rates for the microaluminized 20 μm fine AP matrix relative to its nonaluminized counterpart, when such comparison is possible (Fig. 8). If this is indeed possible with the μAl particles, it would evidently occur with nAl particles, particularly considering the catalytic decomposition of AP with the latter [1,9]. Hence, the burning rates of the nanoaluminized matrices are substantially higher, but less than double, relative to the micron-sized aluminized matrices. This is because of the near-surface heat feedback to the matrix from the nearly complete combustion of the nAl particles soon after their ignition, as suggested previously [22]. These aspects have not been considered in modeling efforts so far and need to be included in the future to determine the propellant burning rate.

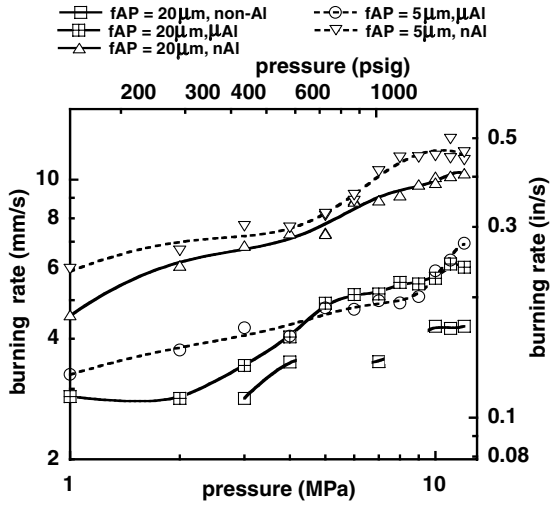

Fig. 8 Burning rates of matrices for 5 μm fine AP.

D. Burning Rates of Propellants

1. Comparison of Present Work with Previous Studies

The results of the nanoaluminized propellant burning rates from the present study are compared in Fig. 9 with those reported with UFAl in recent previous studies on reasonably comparable formulations. The present nanoaluminized formulation with 75 μm fine AP and 450 μm coarse AP is compared with those reported by Dokhan et al. [22] and Galfetti et al. [24], both using UFAl obtained from American and Russian sources, respectively. The corresponding microaluminized propellant burning rates from each of the studies are also shown in that figure to show the increase in the burning rate with use of nano-/ultrafine aluminum instead of microaluminum. Minor variations in total solids loading, binder type, coarse-to-fine AP ratio, coarse and fine AP sizes, and ultrafine/nanoaluminum and microaluminum sizes do inevitably exist across these comparisons. Despite this, it can be seen that all the studies, including the present one, show a 2–3 times increase in the propellant burning rate with the use of nano-/ultrafine aluminum relative to microaluminum.

2. Baseline Formulations

The burning rates of propellants with a bimodal size distribution of AP particles, non-, micro-, and nanoaluminized, are presented in Fig. 10 for two sizes of the fine AP particles, namely 5 and 75 μm. These two fine AP sizes are chosen as baseline formulations because the non- and microaluminized 5 μm fine AP propellants involve plateau-burning characteristics whereas those with the 75 μm fine AP particles do not. This is important because past investigators have reported no effect of nAl on the pressure exponent of the propellant burning rate [23–25]. In fact, the non- and microaluminized 5 μm fine AP propellants have lower burning rates than their 75 μm fine

Table 3 Measured heats of combustion of propellants

S. no.	Propellant	Heat of combustion, MJ/kg
1	Nonaluminized	−6.08
2	Microaluminized	−7.65
3	Nanoaluminized	−7.51

Table 2 Theoretical performance calculations, where c^* is the characteristic velocity.

S. no.	Propellant	Adiabatic flame temperature, K	c^*, m/s	Vacuum specific impulse, s
1	Nonaluminized	2384.47	1333.3	232.1
2	Microaluminized	2937.08	1425.7	258.7
3	Nanoaluminized	2865.73	1405.8	254.9

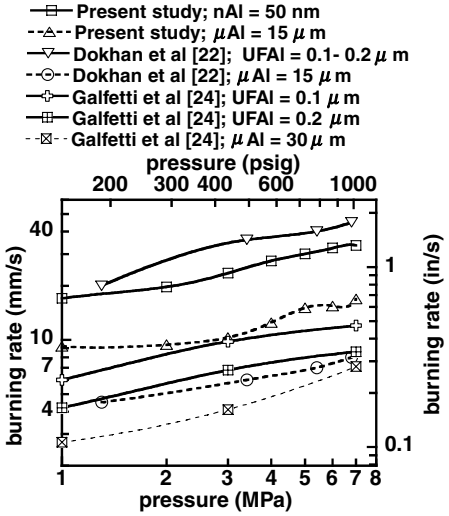

Fig. 9 Comparison of burning rates of propellant formulations between the present study and previous studies. Present study: coarse AP (450 μm)/fine AP (75 μm) = 72/28 = 2.866:1, 15% Al, total solids = 87.5%. Dokhan et al [22]: coarse AP (400 μm)/fine AP (82.5 μm) = 80/20 = 4:1, 18% Al, total solids = 89%. Galfetti et al [24]: coarse AP (150 μm)/fine AP (75 μm) = 80/20 = 4:1, 15% Al, total solids = 83%.

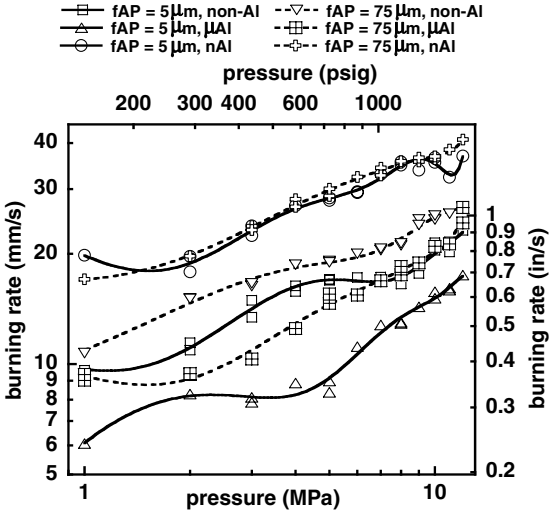

Fig. 10 Burning rates of propellants with 5 and 75 μm fine AP and 450 μm coarse AP particles.

AP counterparts, as shown in Fig. 10. This is contrary to the general expectation of increased burning rates with decreased size of AP particles; this is related to the plateau-burning effects shown by the 5 μm fine AP propellants. The nonaluminized 5 μm fine AP propellant exhibits a plateau-burning-rate trend in the intermediate pressure range; its microaluminized counterpart exhibits a similar trend in a lower pressure range and also at a lower burning-rate level. The microaluminized propellant burning rates are, in general, lower than their nonaluminized counterparts, because the aluminum particles are added in place of coarse AP particles to maintain the total solids loading constant as well as the fine AP/binder matrix ratio. The fine AP/binder ratio is crucial in determining the extinction characteristics of the matrix and is related to plateau burning of the propellant [39,41]. Removing some of the coarse AP in the propellant and replacing it with μAl decreases the number density of the LEFs anchored over the coarse AP/matrix interfaces on the burning surface. The LEFs act as the chief near-surface heat sources that control the burning rate [47]. Besides this, the distance between adjacent coarse particles is increased, which affects the interaction between the adjacent LEFs anchored over them and, hence, the pressure range of their interaction. Because this interaction is responsible for plateau-burning-rate trends, the microaluminized 5 μm fine AP propellant exhibits a plateau in its burning rate in a lower pressure range than its nonaluminized counterpart, as shown in Fig. 10. The plateau effects are nearly absent in the non- and microaluminized propellants with the 75 μm fine AP particles, because the matrices with that size of fine AP particles exhibit no midpressure extinction because of binder-melt flow effects [39]. However, the trend of lower burning rates for the microaluminized propellant than the nonaluminized one is preserved, for the same reason already mentioned.

When the μAl is replaced by nAl, the burning rates are nearly doubled and increase by at least ~50% over the nonaluminized values. The plateaus associated with the binder-melt flow at low-to-intermediate pressures are washed out by addition of the nAl in the case of the 5 μm fine AP propellants. But, the nanoaluminized propellant exhibits a low pressure exponent in the elevated pressure range, above 7 MPa. The increase in the burning rate with the addition of nAl is from its near-complete combustion near the propellant's burning surface [22], as was observed with the fine AP/binder matrix burning rates in Fig. 8 earlier. The washout of the plateaus as already noted and an increase in the propellant burning rates with the addition of nAl indicate that the combustion of nAl is the predominant heat feedback mechanism that controls the burning rate in this case. The low pressure exponent of the nanoaluminized propellant at elevated pressures also points to the diffusion-limited nature of aluminum combustion that is insensitive to pressure in that pressure range. The low pressure exponent was observed in the burning rate of the 5 μm fine AP/binder matrix as well, in the elevated pressure range (Fig. 8). This shows that the mechanism of heat feedback from the nAl combustion controlling the propellant burning rate is independent of the interaction of LEFs over adjacent coarse AP particles that is present in the propellants but absent in the matrix. However, the nanoaluminized 20 μm fine AP/binder matrix burning rates (Fig. 8), though high relative to those of its non- and microaluminized counterparts, does not exhibit a low pressure exponent at elevated pressures unlike in the case of the 5 μm fine AP matrix. This could be due to attachment of LEFs to the larger fine AP particles in this case, which tends to increase the pressure exponent [50,51] in the elevated pressure range.

A similar effect prevails with 75 μm fine AP propellant when nAl is added (Fig. 10). The increase in the burning rate with nAl addition is not accompanied by any significant change in the pressure exponent, as observed by past investigators [23–25]. This has been interpreted previously as due to the kinetically limited combustion of nanoaluminum that controls the propellant burning rate up to intermediate pressures of <7 MPa.

3. *Effect of Fine AP Size*

Retaining the coarse AP size at 450 μm, propellants with two additional fine AP sizes, namely, 20 and 53 μm, are considered to examine the effect of fine AP size on their burning rates, without and with micro- or nanoaluminum. The results of the propellant burning rates for all four fine AP sizes tested are shown separately for the non-, micro-, and nanoaluminized propellants in Fig. 11. The 53 μm fine AP/binder matrix burns by itself in the entire pressure range as is the case with the matrix with the 75 μm fine AP particles (not shown). The most significant observations are as follows.

1) Despite not exhibiting significant plateau effects, the nonaluminized 20 μm fine AP propellant registers lower burning rates than its 5 μm fine AP counterpart. This, in turn, burns slower than the ones with the 53 and 75 μm fine AP (Fig. 11a). This shows that the general trend of finer AP resulting in higher burning rates is not followed with very finely sized AP particles that are susceptible to a significant binder-melt flow effect.

2) The microaluminized 5 and 20 μm fine AP propellants show plateau-burning rates (Fig. 11b), the former in a lower pressure range than the latter. The 20 μm fine AP propellant experiences significant binder-melt flow at higher pressures than the one with 5 μm fine AP [39] and, hence, the observed shift in the plateau trend.

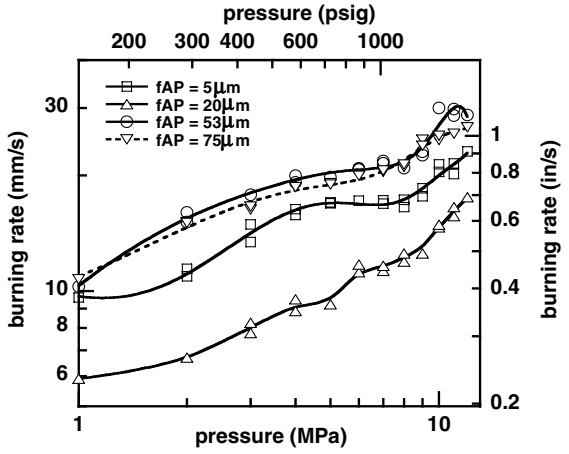

a) Nonaluminized

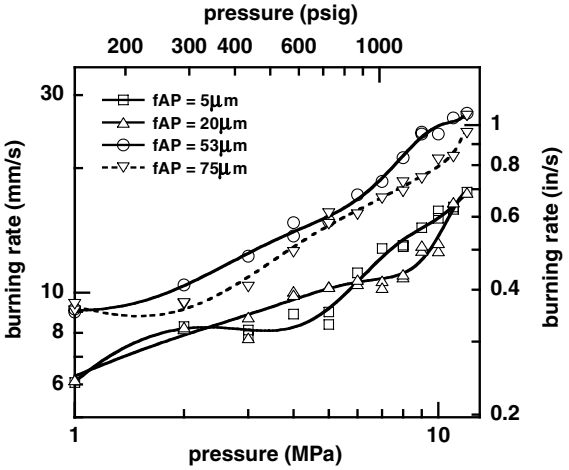

b) Microaluminized

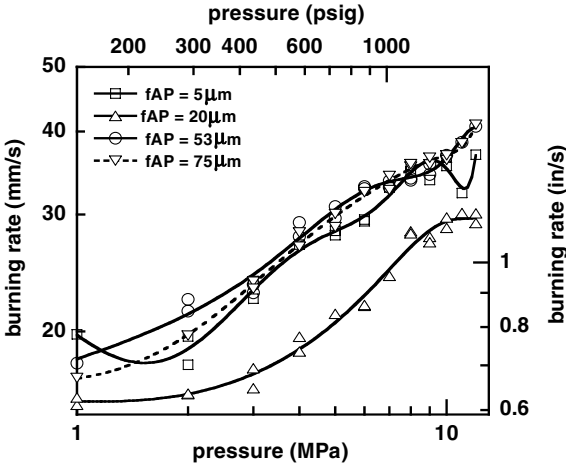

c) Nanoaluminized

Fig. 11 Effect of fine AP particle size on burning rates of propellants with 450 μm coarse AP particles.

3) The nanoaluminized 5 and 20 μm fine AP propellants wash out these plateaus in the low/intermediate pressure ranges (Fig. 11c), as observed earlier. Further, these propellants exhibit low pressure exponents in the elevated pressure range, unlike those with the 53 and 75 μm fine AP particles.

Note that the nanoaluminized 20 μm fine AP/binder matrix does not show the low pressure exponent of the burning rate unlike the 5 μm AP matrix at elevated pressures (Fig. 8). But, both the nanoaluminized propellants with 5 and 20 μm fine AP exhibit such a trend (Fig. 11c). This shows that the presence of the LEFs over the coarse AP particles in the propellant influences the pressure exponent at an elevated pressure. The associated mechanism of the low pressure exponent is the shrinking lateral extent of the LEFs over the coarse particles and the interaction of adjacent ones with an increase in pressure [40]. The outer diffusion flame trailing from the LEFs contributes increasing heat feedback to the burning surface under these conditions. Of course, this mechanism should prevail with the larger-sized fine AP propellants in Fig. 11c, namely, 53 and 75 μm fine AP. But, the attachment of LEFs to the fine particles at elevated pressures noted earlier predominates in these cases to keep the pressure exponent from decreasing in this pressure range.

4. Effect of Coarse AP Size

Perhaps the most instructive result in terms of the combustion mechanism of nanoaluminized propellants is the investigation of the effect of the coarse AP size on the burning rates of the non-, micro-, and nanoaluminized propellant variants. The burning rate of these propellants are shown in Fig. 12 for the two coarse AP sizes, 350 and 250 μm, and for the two fine sizes, 5 and 75 μm. The burning rates for the corresponding sets of propellants, but with coarse AP particles of 450 μm in size, must be included for comparison with Fig. 10. In all the cases, the nanoaluminized propellants show an increase in

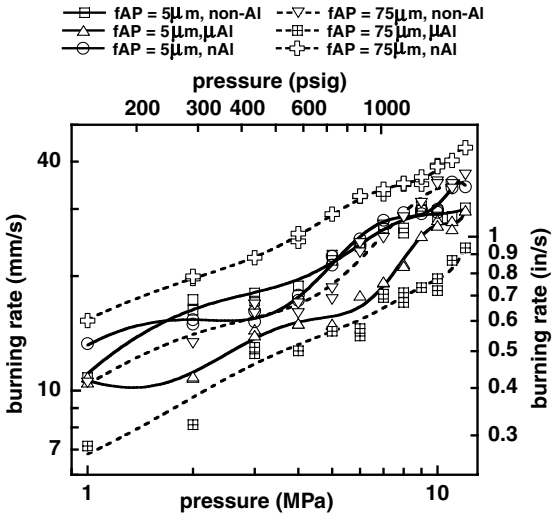

a) Coarse AP size = 350 μm

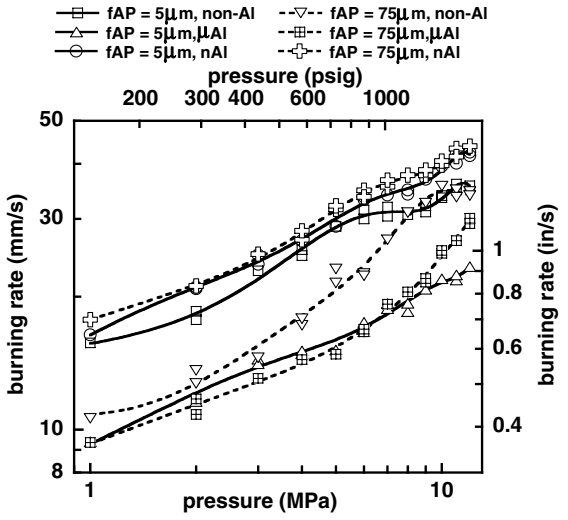

b) Coarse AP size = 250 μm

Fig. 12 Burning rates of propellants with two different coarse AP size particles.

burning rates across the test pressure range over the microaluminized propellants. However, the burning rates of nanoaluminized propellants are observed to be higher relative to their non-/microaluminized counterparts only when the fine AP size is sufficiently large, that is, at 75 μm, with all the coarse AP sizes tested. When the fine AP size is 5 μm, the nanoaluminized propellant burns faster than the non-/microaluminized ones mainly with the 450 μm coarse AP presented earlier (Fig. 10), but not with the 350 and 250 μm coarse AP sizes.

One needs to keep in mind that the removal of coarse AP particles to the extent required to accommodate the nAl should contribute to a decrease in burning rate, as in the case of microaluminized propellants. The LEFs anchored over the coarse AP particles are chiefly responsible for burning-rate control in the latter propellants. Their decreased contribution is more than offset by the near-surface complete combustion of nAl in such propellants presented to the extent that the burning rate is actually controlled by heat feedback from nAl combustion. However, nAl combustion follows only upon its ignition, and LEFs continue to remain a chief source of ignition of aluminum, either micro or nano. In propellants with the 75 μm fine AP, shown in Figs. 10 and 12, LEFs attached to the fine AP particles over most of the pressure range (for such a large size) cause easy ignition of the aluminum particles. This leads to significant heat feedback from their combustion. Hence, the nanoaluminized propellants with fine AP of that size burn faster than their corresponding nonaluminized ones, regardless of the size of the coarse AP particles in them.

However, in nanoaluminized propellant with 5 μm fine AP, the fine AP/binder matrix, where the nAl resides, most probably burns in a premixed flame and does not have LEFs attached to the fine AP particles over the test pressure range. Recall that the nanoaluminized fine AP/binder matrix burns fast by itself when compared with the nonaluminized matrix, which does not burn by itself at all (Fig. 8). Despite this, the propellant with the 250 μm coarse AP particles has smaller patches of the fine AP/binder matrix interspersed between the coarse particles. Hence, the fast burning of the matrix is interrupted by the emergence of too many coarse AP particles too often. Thus, the nanoaluminized propellant with coarse AP particles of that size does not burn considerably faster than its nonaluminized counterpart (Fig. 12), in contrast to the case with the 450 μm coarse AP particles seen earlier (Fig. 10). It is quite likely that more nAl accumulates on the burning surface in the latter case (450 μm coarse AP) because of the large space for the matrix in between the coarse particles (following Cohen's pocket model [52]). Further, the LEFs on the coarse particles are too far apart for the effective ignition of the nAl particles accumulating in between. Despite this, the heat feedback from the nAl that ignited controls the matrix burning rate, and a sufficiently exposed area of the matrix on the burning surface is required for this effect to prevail in the propellant. This is possible only with sufficiently large-sized coarse AP particles.

These results show that the burning rate of nanoaluminized propellants does not increase over nonaluminized ones under all conditions. On the whole, there are multiple physical mechanisms competing for burning-rate control, one among which is the near-surface heat feedback from the nearly complete combustion of nAl following its ignition, in the case of nanoaluminized propellants and matrices. The competing effects of these different mechanisms determine not only the burning rates but also their pressure exponents. Therefore, as can be seen from the present results, the pressure exponents are not always retained with addition of nAl over an expanded test pressure range and with testing at closer pressure intervals than reported in previous works [23–25].

IV. Conclusions

The nAl powder produced from the exploding wire technique in the present work is spherical in shape. WAXD pattern reveals that the purity of the aluminum powder is greater. The nitration rate is relatively greater compare with bulk aluminum. Despite the additional aluminum oxide, because of the enormously large surface area of the nAl, the decrements to the theoretical specific impulse and measured heat of combustion of propellants containing it are minimal relative to those with microaluminized ones. This could be more than offset by the two-phase flow losses with the latter in practice.

The addition of nAl in the fine AP/binder matrix nearly doubles the burning rate when compared with addition of μAl. These results show that the nAl ignites and undergoes near-complete combustion close to the burning surface and, thus, transfers heat by conduction and radiation, thereby increasing the burning rate. The nanoaluminized propellant burning rates are also increased by $\sim$100% relative to microaluminized propellants. Non- and microaluminized propellants containing fine AP of very small size (5 μm) and coarse AP of very large size (450 μm) show plateau-burning-rate trends. These effects are washed out in the corresponding nanoaluminized formulations. The results collectively indicate that the propellant burning rate is controlled by the near-surface nAl combustion, which becomes diffusion limited in the elevated pressure range. These effects show significant changes in the pressure exponent of the burning rate with the addition of nAl over a wider pressure range than tested earlier. With the fine and coarse AP sizes being closer, the plateau-burning effects disappear even with non- and microaluminized formulations, as in routinely used propellants, and the pressure index of the burning rate is then retained with inclusion of nAl, as reported earlier. The predominance of nAl combustion in controlling the propellant burning rate is limited 1) when the exposed areas of the fine AP/binder matrix on the burning surface are restricted by relatively smaller-sized coarse AP particles, and 2) when the fine AP particles are too small to hold attached LEFs and ignite the nAl effectively. Under these conditions, the increase in the burning rate of the nanoaluminized propellant over the nonaluminized one is marginal.

Acknowledgment

This work was supported by the Armament Research Board, India.

References

[1] Romonadova, L. D., and Pokhil, P. K., "Action of Silica on the Burning Rates of Ammonium Perchlorate Compositions," *Fizika Goreniya i Vzryva*, Vol. 6, No. 3, July 1970, pp. 285–290. doi:10.1007/BF00742496

[2] Ivanov, Y. F., Osmonoliev, M. N., Sedoi, V. S., Arkhipov, V. A., Bondarchuk, S. S., Vorozhtsov, A. B., Korotkikh, A. G., and Kuznetsov, V. T., "Productions of Ultra-Fine Powders and Their Use in High Energetic Compositions," *Propellants, Explosives, Pyrotechnics*, Vol. 28, No. 6, 2003, pp. 319–333. doi:10.1002/prep.200300019

[3] Lee, G. H., Park, J. H., Rhee, C. K., and Kim, W. W., "Fabrication of Al Nano Powders by Pulsed Wire Evaporation (PWE) Method," *The Journal of Industrial and Engineering Chemistry*, Vol. 9, No. 1, 2003, pp. 71–75.

[4] Mench, M. M., Kuo, K. K., Yeh, C. L., and Lu, Y. C., "Comparison of Thermal Behaviour of Regular and Ultra-Fine Aluminium Powders (ALEX) Made from Plasma Explosion," *Combustion Science and Technology*, Vol. 135, June 1998, pp. 269–292. doi:10.1080/00102209808924161

[5] Kwok, Q. S. M., Fouchard, R. C., Turcotte, A.-M., Lightfoot, P. D., Bowes, R., and Jones, D. E. G., "Characterization of Aluminum Nanopowder Compositions," *Propellants, Explosives, Pyrotechnics*, Vol. 27, No. 4, 2002, pp. 229–240. doi:10.1002/1521-4087(200209)27:4<229::AID-PRE-P229>3.0.CO;2-B

[6] Johnson, C. E., Fallis, S., Chafin, A. P., Groshens, T. J., Higa, K. T., Ismail, I. M. K., and Hawkins, T. W., "Characterization of Nanometer- to Micron-Sized Aluminum Powders: Size Distribution from Thermogravimetric Analysis," *Journal of Propulsion and Power*, Vol. 23, No. 4, July–Aug. 2007, pp. 669–682. doi:10.2514/1.25517

[7] Kwon, Y.-S., Moon, J.-S., Ilyin, A. P., Gromov, A. A., and Popenko, E. M., "Estimation of the Reactivity of Aluminum Superfine Powders for Energetic Applications," *Combustion Science and Technology*, Vol. 176, No. 2, Feb. 2004, pp. 277–288. doi:10.1080/00102200490255992

[8] Trunov, M. A., Umbrajkar, S. M., Schoenitz, M., Mang, J. T., and Dreizin, E. L., "Oxidation and Melting of Aluminum Nanopowders,"

Journal of Physical Chemistry B, Vol. 110, No. 26, 2006, pp. 13094–13099.
doi:10.1021/jp0614188

[9] Liu, L., Li, F., Tan, L., Ming, L., and Yi, Y., "Effects of Nanometer Ni, Cu, Al, and NiCu Powders on the Thermal Decomposition of Ammonium Perchlorate," *Propellants, Explosives, Pyrotechnics*, Vol. 29, No. 1, 2004, pp. 34–38.
doi:10.1002/prep.200400026

[10] Pivkina, A., Ulyanova, P., Frolov, Y., Zavyalov, S., and Schoonman, J., "Nanomaterials for Heterogeneous Combustion," *Propellants, Explosives, Pyrotechnics*, Vol. 29, No. 1, 2004, pp. 39–48.
doi:10.1002/prep.200400025

[11] DeSena, J. T., and Kuo, K. K., "Evaluation of Stored Energy in Ultrafine Aluminum Powder Produced by Plasma Explosion," *Journal of Propulsion and Power*, Vol. 15, No. 6, Nov.–Dec. 1999, pp. 794–800.
doi:10.2514/2.5498

[12] Trunov, M. A., Schoenitz, M., Zhu, X., and Dreizin, E. L., "Effect of Polymorphic Phase Transformations in Al_2O_3 Film on Oxidation Kinetics of Aluminum Powders," *Combustion and Flame*, Vol. 140, No. 4, March 2005, pp. 310–318.
doi:10.1016/j.combustflame.2004.10.010

[13] Trunov, M. A., Schoenitz, M., and Dreizin, E. L., "Ignition of Aluminum Powders Under Different Experimental Conditions," *Propellants, Explosives, Pyrotechnics*, Vol. 30, No. 1, 2005, pp. 36–43.
doi:10.1002/prep.200400083

[14] Rai, A., Park, K., Zhou, L., and Zachariah, M. R., "Understanding the Mechanism of Aluminum Nano-Particle Oxidation," *Combustion Theory and Modelling*, Vol. 10, No. 5, Oct. 2006, pp. 843–859.
doi:10.1080/13647830600800686

[15] Kwon, Y.-S., Gromov, A. A., Ilyin, A. P., Popenko, E. M., and Rim, G.-H., "The Mechanism of Combustion of Superfine Aluminum Powders," *Combustion and Flame*, Vol. 133, No. 4, June 2003, pp. 385–391.
doi:10.1016/S0010-2180(03)00024-5

[16] Huang, Y., Risha, G. A., Yang, V., and Yetter, R. A., "Combustion of Bimodal Nano/Micron-Sized Aluminum Particle Dust in Air," *Proceedings of the Combustion Institute*, Vol. 31, No. 2, Jan. 2007, pp. 2001–2009.
doi:10.1016/j.proci.2006.08.103

[17] Jones, D. E. G., Turcotte, R., Fouchard, R. C., Kwok, Q. S. M., Turcotte, A.-M., and Abdel-Qader, Z., "Hazard Characterization of Aluminum Nanopowder Compositions," *Propellants, Explosives, Pyrotechnics*, Vol. 28, No. 3, 2003, pp. 120–131.
doi:10.1002/prep.200390018

[18] Kwok, Q. S. M., Badeen, C., Armstrong, K., Turcotte, R., Jones, D. E. G., and Gertsman, V. Y., "Hazard Characterization of Uncoated and Coated Aluminum Nanopowder Compositions," *Journal of Propulsion and Power*, Vol. 23, No. 4, July–Aug. 2007, pp. 659–668.
doi:10.2514/1.25181

[19] Bocanegra, P. E., Chauveau, C., and Gokalp, I., "Experimental Studies on the Burning of Coated and Uncoated Micro- and Nano-Sized Aluminum Particles," *Aerospace Science and Technology*, Vol. 11, No. 1, Jan. 2007, pp. 33–38.
doi:10.1016/j.ast.2006.10.005

[20] Dubois, C., Lafleur, P. G., Roy, C., Brousseau, P., and Stowe, R. A., "Polymer-Grafted Metal Nanoparticles for Fuel Applications," *Journal of Propulsion and Power*, Vol. 23, No. 4, July–Aug. 2007, pp. 651–658.
doi:10.2514/1.25384

[21] Pai Verneker, V. R., Seetharamacharyulu, D., and Mallya, R. M., "Combustion of Ammonium Perchlorate-Aluminum Mixtures," *Journal of Spacecraft and Rockets*, Vol. 16, No. 6, Nov.–Dec. 1979, pp. 436–438.
doi:10.2514/3.28020

[22] Dokhan, A., Price, E. W., Seitzman, J. M., and Sigman, R. K., "The Effects of Bimodal Aluminum with Ultra-Fine Aluminum on the Burning Rates of Solid Propellants," *Proceedings of the Combustion Institute*, Vol. 29, No. 2, 2002, pp. 2939–2945.
doi:10.1016/S1540-7489(02)80359-5

[23] De Luca, L. T., Galfetti, L., Severini, F., Meda, L., Marra, G., Vorozhtsov, A. B., Sedoi, V. S., and Babuk, V. A., "Burning of Nano-Aluminized Composite Rocket Propellants," *Combustion, Explosion, and Shock Waves*, Vol. 41, No. 6, 2005, pp. 680–692.
doi:10.1007/s10573-005-0080-5

[24] Galfetti, L., De Luca, L. T., Severini, F., Meda, L., Marra, G., Marchetti, M., Regi, M., and Bellucci, S., "Nanoparticles for Solid Propellant Combustion," *Journal of Physics: Condensed Matter*, Vol. 18, No. 33, Aug. 2006, pp. S1991–S2005.
doi:10.1088/0953-8984/18/33/S15

[25] Galfetti, L., De Luca, L. T., Severini, F., Colombo, G., Meda, L., and Marra, G., "Pre and Post-Burning Analysis of Nano-Aluminized Solid Rocket Propellants," *Aerospace Science and Technology*, Vol. 11, No. 1, Jan. 2007, pp. 26–32.
doi:10.1016/j.ast.2006.08.005

[26] Pivkina, A. N., Frolov, Yu. V., and Ivanov, D. A., "Nano-Sized Components of Energetic Systems: Structure, Thermal Behavior, and Combustion," *Combustion, Explosion, and Shock Waves*, Vol. 43, No. 1, 2007, pp. 51–55.
doi:10.1007/s10573-007-0008-3

[27] Popenko, E. M., Gromov, A. A., Shamina, Y. Y., Il'in, A. P., Sergienko, A. V., and Popok, N. I., "Effect of the Addition of Ultrafine Aluminum Powders on the Rheological Properties and Burning Rate of Energetic Condensed Systems," *Combustion, Explosion, and Shock Waves*, Vol. 43, No. 1, Jan. 2007, pp. 46–50.
doi:10.1007/s10573-007-0007-4

[28] Dokhan, A., "The Effects of Aluminum Particle Size on Aluminized Propellant Combustion," Ph.D. Dissertation, School of Aerospace Engineering, Georgia Inst. of Technology, Atlanta, GA, July 2002.

[29] Karasev, V. V., Onischuk, A. A., Glotov, O. G., Baklanov, A. M., Maryasov, A. G., Zarko, V. E., Panfilov, V. N., Levykin, A. I., and Sabelfeld, K. K., "Formation of Charged Aggregates of Al_2O_3 Nanoparticles by Combustion of Aluminum Droplets in Air," *Combustion and Flame*, Vol. 138, Nos. 1–2, July 2004, pp. 40–54.
doi:10.1016/j.combustflame.2004.04.001

[30] Ivanov, V., Kotov, Y. A., Samatov, O. H., Bohme, R., Karow, H. V., and Schumacher, G., "Synthesis and Dynamic Compaction of Ceramic Nanopowders by Techniques Based on Electric Pulsed Power," *Nano-Structured Materials*, Vol. 6, Nos. 1–4, 1995, pp. 287–290.
doi: 10.1016/0965-9773(95)00054-2

[31] Sabari Giri, V., Sarathi, R., Chakravarthy, S. R., and Venkataseshaiah, C., "Studies on Production and Characterization of Nano-Al_2O_3 Powder Using Wire Explosion Technique," *Materials Letters*, Vol. 58, No. 6, Feb. 2004, pp. 1047–1050.
doi:10.1016/j.matlet.2003.08.015

[32] Sarathi, R., Chakravarthy, S. R., and Venkataseshaiah, C., "Studies on Generation and Characterization of Nano-Alumina Powder Using Wire Explosion Technique," *International Journal of Nanoscience*, Vol. 3, No. 6, 2004, pp. 819–827.
doi:10.1142/S0219581X04002711

[33] Sindhu, T. K., Chakravarthy, S. R., Jayaganthan, R., and Sarathi, R., "Studies on Generation and Characterization of Nano Aluminium Nitride Through Wire Explosion Process," *Synthesis and Reactivity in Inorganic, Metal-Organic, and Nano-Metal Chemistry*, Vol. 36, No. 1, 2006, pp. 53–58.
doi:10.1080/15533170500471714

[34] Sarathi, R., Sindhu, T. K., and Chakravarthy, S. R., "Generation of Nano-Aluminium Powder Through Wire Explosion Process and Its Characterization," *Materials Characterization*, Vol. 58, No. 2, 2007, pp. 148–155.
doi:10.1016/j.matchar.2006.04.014

[35] Sindhu, T. K., Sarathi, R., and Chakravarthy, S. R., "Generation and Characterization of Nano-Aluminium Powder Obtained Through Wire Explosion Process," *Bulletin of Materials Science*, Vol. 30, No. 2, April 2007, pp. 187–195.
doi:10.1007/s12034-007-0034-5

[36] Sarathi, R., Sindhu, T. K., and Chakravarthy, S. R., "Impact of Binary Gas on Nano-Aluminium Particle Formation Through Wire Explosion Process," *Materials Letters*, Vol. 61, Nos. 8–9, 2007, pp. 1823–1826.
doi:10.1016/j.matlet.2006.07.158

[37] Sindhu, T. K., Sarathi, R., and Chakravarthy, S. R., "Understanding the Nano-Particle Formation by Wire Explosion Process Through Experimental and Modelling Studies," *Nanotechnology*, Vol. 19, No. 2, Jan. 2008.
doi:10.1088/0957-4484/19/02/025703

[38] Mukherjee, D., Sonwane, C. G., and Zachariah, M. R., "Kinetic Monte Carlo Simulation of the Effect of Coalescence Energy Release on the Size and Shape Evolution of Nanoparticles Grown as an Aerosol," *Journal of Chemical Physics*, Vol. 119, No. 6, Aug. 2003, pp. 3391–3404.
doi:10.1063/1.1580098

[39] Chakravarthy, S. R., Seitzman, J. M., Price, E. W., and Sigman, R. K., "Intermittent Burning of Ammonium Perchlorate—Hydrocarbon Binder Monomodal Matrixes, Sandwiches, and Propellants," *Journal of Propulsion and Power*, Vol. 20, No. 1, Jan.–Feb. 2004, pp. 101–109.
doi:10.2514/1.9236

[40] Chakravarthy, S. R., Price, E. W., Sigman, R. K., and Seitzman, J. M., "Plateau Burning Behavior of Ammonium Perchlorate Sandwiches and Propellants at Elevated Pressures," *Journal of Propulsion and Power*,

Vol. 19, No. 1, Jan.–Feb. 2003, pp. 56–65.
doi:10.2514/2.6102

[41] Banerjee, S., and Chakravarthy, S. R., "Ammonium Perchlorate-Based Composite Solid Propellant Formulations with Plateau Burning Rate Trends," *Combustion, Explosion, and Shock Waves*, Vol. 43, No. 4, July 2007, pp. 435–441.
doi:10.1007/s10573-007-0059-5

[42] Cookson, R. A., and Fenn, J. B., "Strand Size and Low Pressure Deflagration Limits in a Composite Propellant," *AIAA Journal*, Vol. 8, No. 5, 1970, pp. 864–866.
doi:10.2514/3.5779

[43] Gordon, S., and McBride, B. J., "Computer Program for Calculation of Complex Chemical Equilibrium Compositions and Applications I. Analysis," NASA Rept. RP-1311, 1994.

[44] Gordon, S., and McBride, B. J., "Computer Program for Calculation of Complex Chemical Equilibrium Compositions and Applications II. User's Manual and Program Description," NASA Rept. RP-1311-P2, 1996.

[45] Kishore, K., Pai Verneker, V. R., and Begum, A. S., "Calorific Values of Composite Solid Propellants," *Thermochimica Acta*, Vol. 54, Nos. 1–2, April 1982, pp. 141–146.
doi:10.1016/0040-6031(82)85072-7

[46] Sambamurthi, J. K., Price, E. W., and Sigman, R. K., "Aluminum Agglomeration in Solid-Propellant Combustion," *AIAA Journal*, Vol. 22, No. 8, Aug. 1984, pp. 1132–1138.
doi:10.2514/3.48552

[47] Price, E. W., "Effect of Multi-Dimensional Flamelets in Composite Propellant Combustion," *Journal of Propulsion and Power*, Vol. 11, No. 4, July–Aug. 1995, pp. 717–728.
doi:10.2514/3.23897

[48] Price, E. W., and Sigman, R. K., "Combustion of Aluminized Solid Propellants," *Solid Propellant Chemistry, Combustion, and Motor Interior Ballistics*, edited by V. Yang, T. Brill, and W. Ren, Vol. 185, Progress in Astronautics and Aeronautics, AIAA, Reston, VA, 2000.

[49] Srinivas, V., and Chakravarthy, S. R., "Computer Model of Aluminum Agglomeration on the Burning Surface of a Composite Solid Propellant," *Journal of Propulsion and Power*, Vol. 23, No. 4, July–Aug. 2007, pp. 728–736.
doi:10.2514/1.24797

[50] Price, E. W., Chakravarthy, S. R., Sambamurthi, J. K., and Sigman, R. K., "The Details of Combustion of Ammonium Perchlorate Propellants: Leading Edge Flame Detachment," *Combustion Science and Technology*, Vol. 138, Nos. 1–6, Sept. 1998, pp. 63–83.
doi:10.1080/00102209808952063

[51] Price, E. W., Sambamurthi, J. K., Sigman, R. K., and Panyam, R. R., "Combustion of Ammonium Perchlorate-Polymer Sandwiches," *Combustion and Flame*, Vol. 63, No. 3, March 1986, pp. 381–413.
doi:10.1016/0010-2180(86)90007-6

[52] Cohen, N. S., "A Pocket Model for Aluminium Agglomeration in Composite Propellants," *AIAA Journal*, Vol. 21, No. 5, May 1983, pp. 720–725.
doi:10.2514/3.8139

S. Son
Associate Editor